

Taming singularities of the diagrammatic many-body perturbation theory

Y. Pavlyukh* and J. Berakdar

Institut für Physik, Martin-Luther-Universität Halle-Wittenberg, 06120 Halle, Germany

A. Rubio

*Max Planck Institute for the Structure and Dynamics of Matter and Center for Free-Electron Laser Science and Department of Physics,
Luruper Chaussee 149, 22761 Hamburg, Germany and
Nano-Bio Spectroscopy Group and ETSF Scientific Development Centre,
Dpto. de Física de Materiales, Universidad del País Vasco,
CFM CSIC-UPV/EHU-MPC and DIPC, E-20018 San Sebastián, Spain*

In a typical scenario the diagrammatic many-body perturbation theory generates asymptotic series. Despite non-convergence, the asymptotic expansions are useful when truncated to a finite number of terms. This is the reason for popularity of leading-order methods such as *GW* approximation in condensed matter, molecular and atomic physics. Emerging higher-order implementations suffer from the appearance of nonsimple poles in the frequency-dependent Green's functions and negative spectral densities making self-consistent determination of the electronic structure impossible. Here a method based on the Padé approximation for overcoming these difficulties is proposed and applied to the Hamiltonian describing a core electron coupled to a single plasmonic excitation. By solving the model purely diagrammatically, expressing the self-energy in terms of combinatorics of chord diagrams, and regularizing the diverging perturbative expansions using the Padé approximation the spectral function is determined self-consistently using 3111 diagrams up to the sixth order.

PACS numbers: 71.10.-w, 31.15.A-, 73.22.Dj

Introduction of the Green's function methods to electronic structure calculations is the most prominent achievement of the field-theoretic methods [1–3] on par with the density functional theory having immediate technological applications [4, 5]. Even in the lowest (beyond the mean field) order one obtains significant improvements of e. g. the band gap through the correlational shifts (Δ). Including higher-order diagrams (vertex corrections) is numerically demanding. However, there are more fundamental obstacles on the way arising

from dealing with *diverging series* as the following consideration illustrates.

Padé approximation— Let $g_{\text{model}}(z) = 1/(z - \epsilon - \Delta - i\eta)$ be a model Green's function (GF), and Δ the energy shift due to some interaction. It can be expanded in terms of the non-interacting GF $g_{\text{model}}^{(0)}(z) = 1/(z - \epsilon - i\eta)$ as geometric series:

$$g_{\text{model}}(z) = \sum_{n=0}^{\infty} \frac{\Delta^n}{(z - \epsilon - i\eta)^{n+1}}. \quad (1)$$

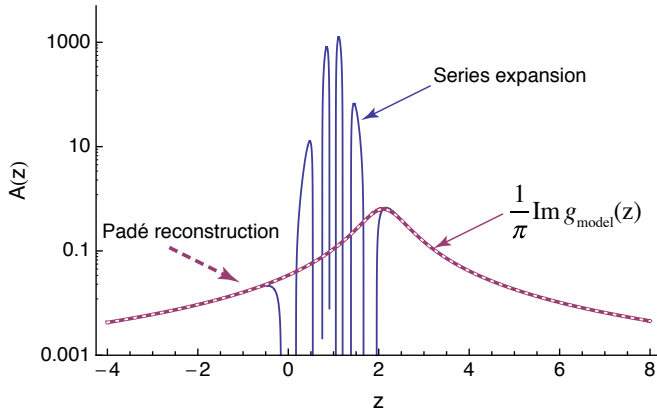


FIG. 1. Reconstruction of $g_{\text{model}}(z)$ from its series expansion (1) in terms of $g_{\text{model}}^{(0)}(z)$ using the Padé approximation. Parameters are as follows: $\Delta = 1.1$, $\epsilon = 1$, $\eta = 0.5$. The series expansion (1) is restricted at $n_{\text{max}} = 10$, and the Padé approximation is applied at the point $z = 6$. Notice that the original (magenta) and reconstructed (white) densities of states are practically indistinguishable.

The series expansion behaves oscillatory in the vicinity of the pole and approaches the original function at large z , i. e., for $|\frac{\Delta}{z - \epsilon - i\eta}| < 1$. Nonetheless, a sensible spectral function, $A(z) = \frac{1}{\pi} \text{Im} g(z)$, in the domain of interest can be reconstructed by using the Padé approximation. The procedure is outlined at Fig. 1 where the original function $g_{\text{model}}(z)$, series expansion (1) and the Padé reconstruction are shown. The Padé approximation allows to obtain very accurate values also in the domain where the series (1) is diverging. The method works so well here because it is known in advance that GF consists of one pole only and this fact is used for the reconstruction (according to the exact form of $g_{\text{model}}(z)$ we use the $[0/1]$ approximant [6]). For realistic calculations we do not have this knowledge and have to rely on some additional assumptions about the analytic structure of the Green's function. As an illustration let us consider the electron-boson Hamiltonian — an ubiquitous in condensed matter physics model.

Model specification and known results— Consider a set of fermionic and bosonic quantum numbers and the associated creation and annihilation operators with standard commutation rules:

$$[c_a, c_b^\dagger]_+ = \delta_{ab}, \quad [a_i, a_j^\dagger]_- = \delta_{ij}. \quad (2)$$

* yaroslav.pavlyukh@physik.uni-halle.de

The model becomes non-trivial when a coupling between fermionic and bosonic degrees of freedom is introduced $\mathcal{H}_I = \sum_{ab} \sum_i \Gamma_{ab}^\dagger c_a^\dagger c_b a_i + \text{H.c.}$ This very general model covers various physical scenarios: (i) interaction of electrons in solids with *real* bosonic excitation such as phonons forming the basis of the polaron model (Sec 4.3 of Mahan [7]), novel applications include quantum dots coupled to nanomechanical oscillators [8]; (ii) electronic excitations such as plasmons under some assumptions mediate the electron-electron interaction. This scenario was first introduced in the work of Lundqvist [9] who considered coupling of the deep hole to plasmonic excitations in metals with well known analytic solution [10–12]. Another prominent example is the photoemission process where the photoelectron interacts with the density fluctuations of the target system [13]; (iii) auxiliary bosonic degrees of freedom is a mathematical trick used to treat a pure electronic Hamiltonian such as the mixed-valence Hamiltonian, i. e. large- U Anderson model (*slave-boson* approach) [14].

Besides the form of the Hamiltonian, it is the notion of the ground state that determines the diagrammatic structure of the model. For instance, the no-hole state is of relevance for the x-ray absorption in the Lundqvist model, while for the photoemission one considers a state with exactly one deep hole. At variance, the ground state of the large- U Anderson model is determined as a state in which the sum of boson and fermion occupation numbers at each site is unity. For this two-component fermionic model very different diagrams (non-crossing approximation) are relevant [15].

Consider the electron-boson Hamiltonian in its simplest form:

$$\mathcal{H} = \epsilon c^\dagger c + c c^\dagger \gamma (a + a^\dagger) + \Omega a^\dagger a, \quad (3)$$

where c is the creation operator of the deep hole with energy ϵ , a^\dagger is the bosonic creation operator of the plasmon with the energy Ω . The facts that there might be several kind of fermions as in the mixed-valence impurity model or the plasmon dispersion are neglected here. However, the generalization to the latter case is possible and will be commented on after the presentation of the diagrammatic solution. The Hamiltonian (3) is quite versatile and is applicable to other scenarios such as resonant-tunneling through a single level coupled to wide-band phonons [16]. Remarkably, also the two particle GF can be found analytically [17], the model can be solved at finite temperatures, and its non-equilibrium properties have also been studied thoroughly [18, 19].

Let us consider the following Green's function

$$g(t - t') = -i \langle \psi | T [c(t) c^\dagger(t')] | \psi \rangle,$$

where $|\psi\rangle$ is the exact ground state of the *no-hole* system. It can be diagrammatically found by writing the cumulant expansion for the Green's function $g(t) = g^{(0)}(t) e^{C(t)}$. Observing that only a single diagram contributes to the *cumulant function* results in

$$C(t) = -\left(\frac{\gamma}{\Omega}\right)^2 (1 + i\Omega t - e^{i\Omega t}). \quad (4)$$

Corresponding exact spectral function is depicted at Fig. 2 together with the zeroth order and spectral function from the

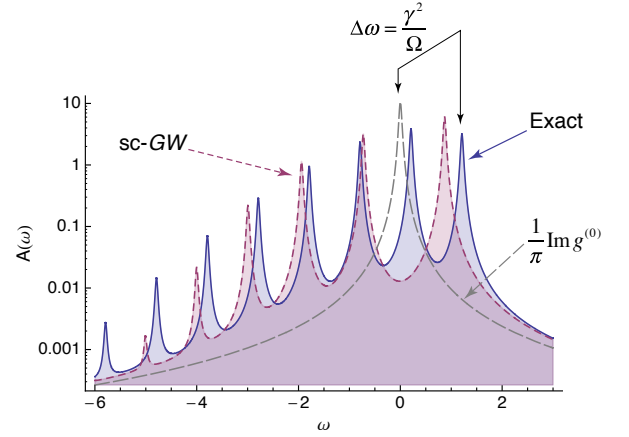


FIG. 2. (Color online) Spectral function at following values of parameters $\epsilon = 0$, $\Omega = 1$, $\gamma = 1.1$, $\eta = 0.03$ and different levels of theory: exact (full line), self-consistent first-order (short dashes), zeroth iteration (long dashes). Shaded areas are equal to unity.

self-consistent GW calculation (sc- GW). The results are plotted for a strongly correlated regime ($\gamma > \Omega$) and can be characterized as follows: (i) The spectral function consist of a main peak shifted by the energy $\Delta\omega = \frac{\gamma^2}{\Omega}$ compared to the noninteracting case; (ii) the quasiparticle peak is followed by the ladder of plasmonic satellites; (iii) the self-consistent GW method predicts the satellites. However, the position of even the main peak is wrong. This inaccuracy is the main motivation for performing higher-order diagrammatic calculations.

Diagrammatic properties— Because the ground state is a no-hole state $c^\dagger|\psi\rangle$ vanishes and, hence, the non-interacting time-ordered Green's function only consists of the hole propagator: $g^{(0)}(t - t') = i\theta(t' - t)e^{-i\epsilon(t-t')}$. This fact simplifies the diagrams considerably: (i) in the expansion for the Green's function (g) and the self-energy (Σ) all intermediate points are time-ordered (Fig. 3); (ii) diagrams containing loops necessarily yield a zero contribution. These properties allow to write the self-energy for this model explicitly. Because there is no spatial degrees of freedom the problem is similar to that of the Feynman diagrams enumeration which can be solved by collapsing the space-time variables to one point (the zero-dimensional model [20, 21]). Already such simplified model has interesting applications for correlated electronic calculations in realistic systems [22–24]. Here, we present an analytic solution of a more complicated one-dimensional case.

Let $\Sigma^{(n,\alpha)}(\omega)$ be an n th-order self-energy term corresponding to a particular diagram which will be denoted as α . We will prove below that the corresponding expression in the frequency representation is given by the product:

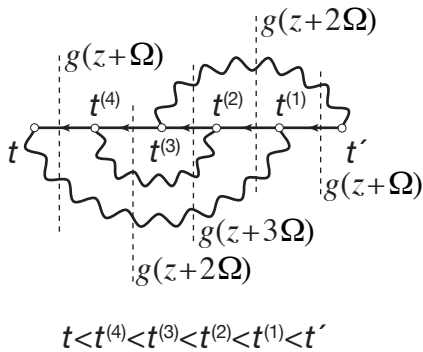
$$\Sigma^{(n,\alpha)}[g; \omega] = (\gamma^2)^n \prod_{i=1}^{2n-1} g(\omega + k_i^{(n,\alpha)}\Omega), \quad (5)$$

where the integer number of absorbed plasmons in each fermionic line ($k_i^{(n,\alpha)}$) is computed as a number of bosonic lines crossing each vertical line (Fig. 3). $2n - 1$ vertical lines

are positioned such that they cut each fermionic line. This equation can be derived by using the nonequilibrium Green's function formalism. Let a vertical line separate times lying on the forward and backward branches of the Keldysh contour in an expression for the *lesser* self-energy ($\Sigma^<$). Consider, for instance, a third vertical line at Fig. 3. It contributes $g^<(z - y_1 - y_2 - y_3)W^<(y_1)W^<(y_2)W^<(y_3)$ to $\Sigma^<$. Here, $W^<(y) = \gamma^2\delta(y + \Omega)$ is the lesser bosonic propagator. Performing three frequency integrals (over y_1, y_2, y_3) a contribution proportional to $g^<(z + 3\Omega)$ is obtained. Similar considerations can be repeated for each vertical line and fermionic propagator yielding in total $2n - 1$ terms for each n th-order self-energy diagram $\Sigma^<(z) = \sum_{i=1}^{2n-1} f_i(z)g^<(z + k_i\Omega)$. Now, since $f_i(z)$ are non-singular the generic expression for the time-ordered self-energy (5) is obtained.

Expansion (5) is a new exact result for the S -model which also permits generalizations for more general scenarios. Electronic spectra of numerous realistic materials have been rationalized in terms of the time-ordered [25–28] or retarded [29] cumulant expansions, which as we have seen above, are exact for the considered model. The presence of multiple plasmonic satellites is a marked feature of these materials [29–33]. The plasmon dispersion is the only modification needed for generalization to this case. It amounts to introducing additional sums over the plasmonic momentum at each vertex, but does not change the diagrammatic structure. A viable route to use present results for the momentum-resolved calculations is via the GF momentum average approximation [34]. It was demonstrated to yield an accurate description of dressed particles in the Holstein polaron model [35].

Eq. (5) serves as the starting point for numerics; complexity goes into the generation of Feynman diagrams and determination of the coefficients $k_i^{(n,\alpha)}$. This is the second important ingredient of our approach. The coefficients are computed purely algebraically by computing variational derivatives of fermionic and bosonic propagators [36] with respect to the external position and time-dependent potential $\phi(1)$ (for simplicity time variables are denoted as $t_i \equiv i$). $\Sigma[G, W]$ can be ob-



$$\Sigma(z) = (\gamma^2)^3 g(z + \Omega)g(z + 2\Omega)g(z + 3\Omega)g(z + 2\Omega)g(z + \Omega)$$

FIG. 3. Example of the self-energy in time domain. The system only contains holes. Therefore there is only one possible time-ordering as shown below the diagram. Bosonic propagators are denoted as wavy-lines.

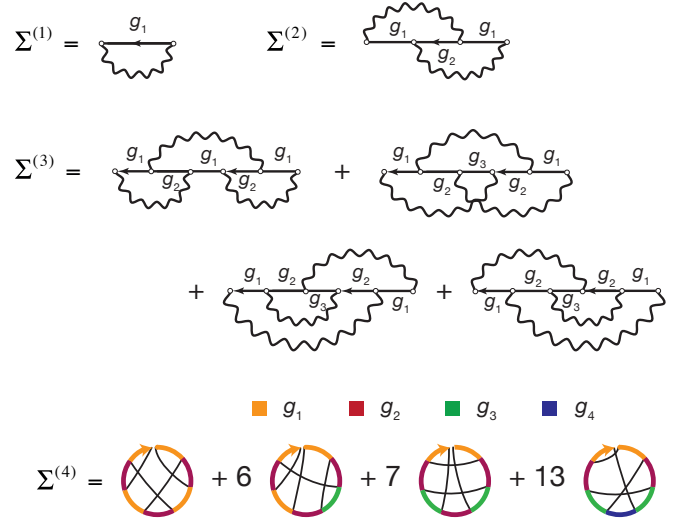


FIG. 4. Four lowest orders of the diagrammatic expansion of the self-energy for the S -model in frequency space. Notice that two diagrams of the third-order containing loops are not shown because they are equal to zero. The fourth-order self-energy is given in terms of chord diagrams with color-coding. Only one representative for each class is shown. Due to the absence of loops an isomorphism between the Feynman diagrams and the chord diagrams can be established.

tained by iterating a set of the Hedin's equations [37]. As was shown above the bosonic propagator in the present model does not renormalize (loops give zero contribution), i. e. $\frac{\delta W(12)}{\delta \phi(3)} = 0$, leading to a simpler set of equations:

$$\Gamma(12, 3) = \delta(12)\delta(13) + \frac{\delta \Sigma(12)}{\delta V(3)}, \quad (6a)$$

$$\Sigma(12) = i \int W(13)G(14)\Gamma(42, 3)d(34), \quad (6b)$$

$$\frac{\delta G(12)}{\delta V(3)} = \int G(14)G(52)\Gamma(45, 3)d(45), \quad (6c)$$

where $\Gamma(12, 3)$ is the vertex function, $\Sigma(12)$ is the electron self-energy, and $V(3)$ is the external $[\phi(3)]$ plus the induced field in the system. All these quantities are functionally dependent on the external field $\phi(3)$ and on the full electron propagator $G(12)$. The set of equations (6) can now be iterated starting from $\Gamma^0(12, 3) = \delta(12)\delta(13)$ leading to the diagrams shown at Fig. 4.

The chord diagram [38, 39] representation is natural in this case because according to the analysis above the fermionic loops yield zero contribution. In order to further facilitate the interpretation of the graphs in frequency space we use color coding for the coefficients $k_i^{(n,\alpha)}$ entering the GF arguments. The graphs were generated by our symbolic algorithm in MATHEMATICA computer algebra system. Conversion from the time to frequency domains is likewise performed using a symbolic algorithm. The self-energy accurate to the sixth order comprises 1, 1, 4, 27, 248, and 2830 diagrams of the first to sixth orders, respectively, and has the following algebraic

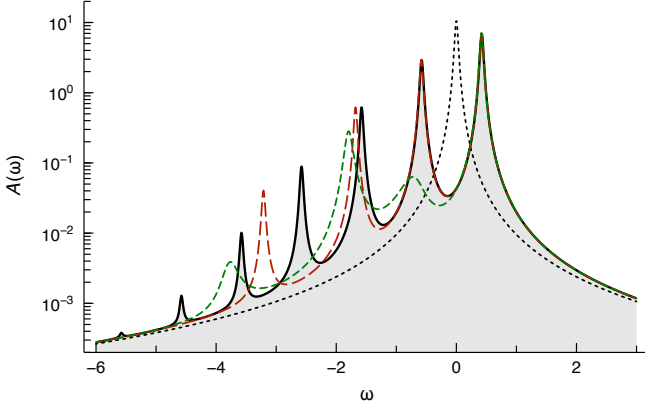


FIG. 5. Spectral function of the S -model at different levels of the theory: exact (full line), self-consistent third-order (short dashed), sixth-order (long dashed), zeroth iteration (dotted) for the following values of parameters: $\epsilon = 0$, $\Omega = 1$, $\gamma = 0.65$, $\eta = 0.03$.

representation:

$$\begin{aligned} \Sigma = & \alpha g_1 + \alpha^2 g_2 g_1^2 + \alpha^3 (g_2^2 g_1^3 + 3g_2^2 g_3 g_1^2) \\ & + \alpha^4 (g_2^3 g_1^4 + 6g_2^3 g_3 g_1^3 + 7g_2^3 g_3^2 g_1^2 + 13g_2^2 g_3^2 g_4 g_1^2) \\ & + \alpha^5 (g_2^4 g_1^5 + 9g_2^4 g_3 g_1^4 + 23g_2^4 g_3^2 g_1^3 + 26g_2^3 g_3^2 g_4 g_1^3 \\ & + 15g_2^4 g_3^3 g_1^2 + 58g_2^3 g_3^3 g_4 g_1^2 + 45g_2^2 g_3^3 g_4^2 g_1^2 + 71g_2^2 g_3^2 g_4^2 g_5 g_1^2) \\ & + \alpha^6 (g_1^6 g_2^5 + 12g_1^5 g_2^5 g_3 + 48g_1^4 g_2^5 g_3^2 + 72g_1^3 g_2^5 g_3^3 \\ & + 31g_1^2 g_2^5 g_3^4 + 39g_1^4 g_2^4 g_3^2 g_4 + 194g_1^3 g_2^4 g_3^3 g_4 + 183g_1^2 g_2^4 g_3^4 g_4 \\ & + 90g_1^3 g_2^3 g_3^3 g_4^2 + 313g_1^2 g_2^3 g_3^4 g_4^2 + 145g_1^2 g_2^2 g_3^4 g_4^3 \\ & + 142g_1^3 g_2^3 g_3^2 g_4^2 g_5 + 310g_1^2 g_2^3 g_3^3 g_4^2 g_5 + 470g_1^2 g_2^2 g_3^3 g_4^3 g_5 \\ & + 319g_1^2 g_2^2 g_3^3 g_4^2 g_5^2 + 461g_1^2 g_2^2 g_3^2 g_4^2 g_5^2 g_6) + O(\alpha^7), \end{aligned} \quad (7)$$

where $g_k \equiv g(\omega + k\Omega)$ and $\alpha \equiv \gamma^2$. Setting all $g_k \equiv 1$ a generating function for the enumeration of all chord diagrams is obtained:

$$y(\alpha) = \alpha + \alpha^2 + 4\alpha^3 + 27\alpha^4 + 248\alpha^5 + 2830\alpha^6 + O(\alpha^7),$$

which also fulfills the following ordinary differential equation $2\alpha^2 y \frac{dy}{d\alpha} + \alpha y^2 - y + 1 = 0$, resulting from (6) by collapsing all time variables to one point [21].

Our explicit form for the self-energy dictates that the singularities of Σ should be located exactly at the Green's function poles. Physically it is wrong as it is well known that the self-energy poles lie between the poles of the corresponding exact Green's function [40]. These two facts can be reconciled noticing that already starting with the second order

$$\Sigma^{(2)}(\omega) = (\gamma^2)^2 g(\omega + \Omega)g(\omega + 2\Omega)g(\omega + \Omega)$$

the self-energy contains *higher-order* poles in the frequency domain. As in our toy model (Fig. 1) they are responsible for the energy shift.

Application to the S -model—Assume that in the course of a self-consistent calculation an approximation for the Green's function has been obtained ($g^{(i)}(\omega)$). Using the diagrammatic

expansion viz. Eq. (7) we compute an approximation to the self-energy $\Sigma[g^{(i)}](\omega^*)$ at a chosen frequency point. The point ω^* should belong to the domain where the perturbative expansion converges. In order to obtain the self-energy in the vicinity of Green's function poles where the series diverge we perform the Padé approximation $\Sigma[g^{(i)}](\omega^*) \rightarrow \tilde{\Sigma}^{(i)}(\omega)$ and use the new self-energy in order to update the Green's function according to the Dyson equation $g^{(i+1)}(\omega) = [\omega - \epsilon - \tilde{\Sigma}^{(i)}(\omega)]^{-1}$. Iterations are started from the noninteracting GF $g^{(0)}(\omega) = (\omega - \epsilon - i\eta)^{-1}$ and typically converge within some tens of cycles. The quality of the resulting spectral function strongly depends on the order of perturbative expansions and on the strength of the electron-plasmon scattering γ . For the weakly correlated regime $\gamma \simeq 0.1\Omega$ already the GW approximation faithfully reproduces the exact spectral function. This approximation ceases to be valid in the *correlated regime* as Fig. 2 demonstrates. The energy of the main quasiparticle (QP) peak is the major discrepancy. However, for $\gamma = 0.65$ already third-order treatment yields very good results for QP energy and strength (Fig. 5, short dashed line). The first satellite, which has a rather large contribution to the density of states at this value of γ (notice logarithmic scale), represents a substantially more complicated feature. It can only be captured with a self-energy that is accurate to the 6th order (long dashed line). However, even 3111 diagrams are not sufficient to reproduce the second-order satellite! For realistic systems methods based on the notion of four-point vertex Γ [41, 42] might be a viable alternative. In full generality $\Gamma(12, 34)$ can be obtained by solving a set of coupled Bethe-Salpeter equations in particle-particle ([12]) and particle-hole ([14] and [13]) channels known as parquet equations [2, 43, 44]. If only one such channel is considered one arrives at the so-called T -matrix approximations (TMA) [45, 46] known to complement the GW -approximation [47–52]. We have verified that omitting 22 and 714 diagrams of the 5th and 6th orders from Eq. (7) according to the parquet procedure with only one simple four-vertex does not deteriorate the quality of the results. Even better description of higher order satellites can be expected if the parquet procedure is iterated further.

Conclusions— It is more than computational complexity that prevents applications of many-body perturbation theory beyond the leading order. Resulting asymptotic series lead to Green's functions with incorrect physical properties: non-positive densities, higher-order poles already for the second order [53, 54]. For various statistical models the Padé approximation has been used to extend perturbative expansions beyond their domain of convergence [55]. The same mathematical approach is used here in a different context, to regularize the electron self-energy. With the help of nonequilibrium Green's function theory we have derived the self-energy of the S -model explicitly and demonstrated a connection of its diagrammatic expansion to a certain class of chord diagrams. With the help of the developed symbolic algorithm analytical expressions up to the sixth order in the electron-plasmon interaction are generated. For $\omega^* \gg \frac{\gamma^2}{\Omega}$ the series converge rapidly, however, there are no interesting spectral features in this domain. Therefore, to recursively update the Green's function in the whole spectral range the self-energy is regularized before

plugging it into the Dyson equation. In this way, even in the correlated regime ($\gamma = 0.65\Omega$) the present approach allows to accurately describe the QP peak and the first-order satellite. Hence, the Padé approximation makes self-consistent calculations with higher order vertex function feasible.

ACKNOWLEDGMENTS

YP and JB acknowledge financial support of the German Research Foundation (DFG) through SFB 762 and PA 1698/1-1 projects. AR acknowledges financial support from the European Research Council Advanced Grant DY-Namo (ERC-2010- AdG-267374), Spanish Grant (FIS2013-46159-C3-1-P), Grupos Consolidados UPV/EHU del Gobierno Vasco (IT578-13) and European Community FP7 project CRONOS (Grant number 280879-2) and COST Actions CM1204 (XLIC) and MP1306 (EUSpec).

-
- [1] P. Nozières and D. Pines, *The theory of quantum liquids*, Advanced book classics (Westview Press, Perseus Books Group, Boulder, CO, 1999).
 - [2] A. O. Gogolin, A. A. Nersisyan, and A. M. Tsvelik, *Bosonization and strongly correlated systems* (Cambridge University Press, Cambridge, U.K.; New York, NY, 1998).
 - [3] G. Giuliani and G. Vignale, *Quantum theory of the electron liquid* (Cambridge University Press, Cambridge, UK, 2005).
 - [4] R. M. Dreizler and E. K. U. Gross, *Density Functional Theory an Approach to the Quantum Many-Body Problem* (Springer Berlin Heidelberg, Berlin, Heidelberg, 1990).
 - [5] G. Onida, L. Reining, and A. Rubio, *Rev. Mod. Phys.* **74**, 601 (2002).
 - [6] The Padé approximation has form of rational function (denoted as $[M/N]$) with $M + N + 1$ coefficients, M, N are the orders of the numerator and denominator, respectively.
 - [7] G. Mahan, *Many-particle physics*, 3rd ed. (Kluwer Academic/Plenum Publishers, New York, 2000).
 - [8] M. Tahir, A. MacKinnon, and U. Schwingenschlögl, *Scientific Reports* **4**, 4035 (2014).
 - [9] B. I. Lundqvist, *Phys. Kondens. Mater.* **9**, 236 (1969).
 - [10] D. C. Langreth, *Phys. Rev. B* **1**, 471 (1970).
 - [11] C. O. Almbladh and P. Minnhagen, *Phys. Rev. B* **17**, 929 (1978).
 - [12] M. Cini and A. D'Andrea, *J. Phys. C* **21**, 193 (1988).
 - [13] L. Hedin, J. Michiels, and J. Inglesfield, *Phys. Rev. B* **58**, 15565 (1998).
 - [14] P. Coleman, *Phys. Rev. B* **29**, 3035 (1984).
 - [15] N. S. Wingreen and Y. Meir, *Phys. Rev. B* **49**, 11040 (1994).
 - [16] N. S. Wingreen, K. W. Jacobsen, and J. W. Wilkins, *Phys. Rev. Lett.* **61**, 1396 (1988).
 - [17] N. S. Wingreen, K. W. Jacobsen, and J. W. Wilkins, *Phys. Rev. B* **40**, 11834 (1989).
 - [18] L. K. Dash, H. Ness, and R. W. Godby, *J. Chem. Phys.* **132**, 104113 (2010).
 - [19] H. Ness, L. K. Dash, M. Stankovski, and R. W. Godby, *Phys. Rev. B* **84**, 195114 (2011).
 - [20] L. G. Molinari, *Phys. Rev. B* **71**, 113102 (2005).
 - [21] Y. Pavlyukh and W. Hübner, *J. Math. Phys.* **48**, 052109 (2007).
 - [22] G. Lani, P. Romaniello, and L. Reining, *New J. Phys.* **14**, 013056 (2012).
 - [23] J. A. Berger, P. Romaniello, F. Tandetzky, B. S. Mendoza, C. Brouder, and L. Reining, *New J. Phys.* **16**, 113025 (2014).
 - [24] A. Stan, P. Romaniello, S. Rigamonti, L. Reining, and J. A. Berger, arXiv:1503.07742v2 (2015).
 - [25] F. Aryasetiawan, L. Hedin, and K. Karlsson, *Phys. Rev. Lett.* **77**, 2268 (1996).
 - [26] B. Holm and F. Aryasetiawan, *Phys. Rev. B* **56**, 12825 (1997).
 - [27] M. Guzzo, G. Lani, F. Sottile, P. Romaniello, M. Gatti, J. J. Kas, J. J. Rehr, M. G. Silly, F. Sirotti, and L. Reining, *Phys. Rev. Lett.* **107**, 166401 (2011).
 - [28] Y. Pavlyukh, A. Rubio, and J. Berakdar, *Phys. Rev. B* **87**, 205124 (2013).
 - [29] J. J. Kas, J. J. Rehr, and L. Reining, *Phys. Rev. B* **90**, 085112 (2014).
 - [30] J. Lischner, D. Vigil-Fowler, and S. G. Louie, *Phys. Rev. Lett.* **110**, 146801 (2013).
 - [31] M. Guzzo, J. J. Kas, L. Sponza, C. Giorgetti, F. Sottile, D. Pierucci, M. G. Silly, F. Sirotti, J. J. Rehr, and L. Reining, *Phys. Rev. B* **89**, 085425 (2014).
 - [32] J. Lischner, D. Vigil-Fowler, and S. G. Louie, *Phys. Rev. B* **89**, 125430 (2014).
 - [33] J. J. Kas, F. D. Vila, J. J. Rehr, and S. A. Chambers, *Phys. Rev. B* **91**, 121112 (2015).
 - [34] M. Berciu and G. L. Goodvin, *Phys. Rev. B* **76**, 165109 (2007).
 - [35] M. Berciu, *Phys. Rev. Lett.* **97**, 036402 (2006).
 - [36] G. Strinati, *Riv. Nuovo Cimento* **11**, 1 (1988).
 - [37] L. Hedin, *Phys. Rev.* **139**, A796 (1965).
 - [38] V. Pilaud and J. Rué, *Adv. Appl. Math.* **57**, 60 (2014).
 - [39] V. Hinich and A. Vaintrob, *Selecta Math. (N.S.)* **8**, 237 (2002).
 - [40] J. Winter, *Nucl. Phys. A* **194**, 535 (1972).
 - [41] J. P. Blaizot and G. Ripka, *Quantum theory and finite systems* (Cambridge, MA, 1986).
 - [42] R. van Leeuwen, N. E. Dahlen, and A. Stan, *Phys. Rev. B* **74**, 195105 (2006).
 - [43] B. Roulet, J. Gavoret, and P. Nozières, *Phys. Rev.* **178**, 1072 (1969).
 - [44] G. Rohringer, A. Valli, and A. Toschi, *Phys. Rev. B* **86**, 125114 (2012).
 - [45] P. Romaniello, F. Bechstedt, and L. Reining, *Phys. Rev. B* **85**, 155131 (2012).
 - [46] D. Peng, S. N. Steinmann, H. v. Aggelen, and W. Yang, *J. Chem. Phys.* **139**, 104112 (2013).
 - [47] S. Nagano, K. S. Singwi, and S. Ohnishi, *Phys. Rev. B* **29**, 1209 (1984).
 - [48] C. Verdozzi, R. W. Godby, and S. Holloway, *Phys. Rev. Lett.* **74**, 2327 (1995).
 - [49] I. A. Nechaev and E. V. Chulkov, *Phys. Rev. B* **71**, 115104 (2005).
 - [50] Z. Qian, *Phys. Rev. B* **73**, 035106 (2006).
 - [51] M. Puig von Friesen, C. Verdozzi, and C.-O. Almbladh, *Phys. Rev. Lett.* **103**, 176404 (2009).
 - [52] Y. Yang, H. v. Aggelen, S. N. Steinmann, D. Peng, and W. Yang, *J. Chem. Phys.* **139**, 174110 (2013).

- [53] G. Stefanucci, Y. Pavlyukh, A.-M. Uimonen, and R. van Leeuwen, Phys. Rev. B **90**, 115134 (2014).
- [54] A.-M. Uimonen, G. Stefanucci, Y. Pavlyukh, and R. van Leeuwen, Phys. Rev. B **91**, 115104 (2015).
- [55] H. Kleinert, *Critical properties of φ_4 -theories* (World Scientific, River Edge, NJ, 2001).